ELSEVIER

Journal of Molecular Catalysis A: Chemical 119 (1997) 155–163

JOURNAL OF MOLECULAR CATALYSIS A: CHEMICAL

Laser induced desorption of NO from NiO(100): Characterization of potential energy surfaces of excited states

T. Klüner [a,*], H.-J. Freund [b], J. Freitag [c], V. Staemmler [c]

[a] *Lehrstuhl für Physikalische Chemie I, Ruhr-Universität Bochum, Universitätsstr. 150, 44780 Bochum, Germany*
[b] *Fritz-Haber-Institut de Max-Planck-Gesellschaft, Faradayweg 4–6, 14195 Berlin, Germany*
[c] *Lehrstuhl für Theoretische Chemie, Ruhr-Universität Bochum, Universitätsstr. 150, 44780 Bochum, Germany*

Received 26 June 1996; accepted 27 September 1996

Abstract

In order to interpret experimental results such as velocity flux distributions and rotational/vibrational populations of the state resolved UV-laser induced desorption of NO from NiO(100) ab initio calculations at the configuration interaction (CI) and complete active space self consistent field (CASSCF) levels have been performed for the electronic ground state and those excited states which are important for the desorption process. The NO/NiO(100) system was described by a NiO_5^{8-}-cluster embedded in a Madelung field of point charges with NO adsorbed in the on-top position on the central Ni^{2+} ion. Two-dimensional potential energy surfaces for several electronic states have been calculated as a function of the N–Ni distance and the tilt angle of NO towards the surface normal. The excited states involved in the desorption process are charge transfer states in which one electron is transferred from the oxygen 2p-shell into the NO 2π-orbitals. The dependence of the potential energy surfaces on the N–Ni distance is dominated by a strong Coulomb attraction between the NO^- ion formed as an intermediate and the hole created within the cluster. The angular dependence of the potentials favours an upright adsorption geometry if NO^- is approaching the surface. This offers an explanation of the strong coupling between translation and rotation, which has been observed experimentally for the system NO/NiO(100), as well as the absence of such a coupling in the system NO/NiO(111).

1. Introduction

The laser induced desorption of small molecules from well characterized surfaces can be regarded as one of the most elementary steps in surface photochemistry. Detailed experimental investigations have been performed during the last decade in which the desorbing molecules are detected state selectively [1–7]. In most cases metal substrates have been used in the experiments, but the laser induced desorption from oxide surfaces gains interest [8,9] and even stereodynamical information about the desorbing molecules has been obtained recently [10].

Despite the great amount of experimental data there is currently no generally accepted model for the desorption process. Therefore, it is necessary to combine experimental results with theoretical investigations in order to get a detailed mechanistic understanding of the desorption process at a microscopic level.

A theoretical description requires the calculation of sufficiently accurate potential energy surfaces for the states involved in the desorption

* Corresponding author.

PII S1381-1169(96)00479-7

process as a function of those internal degrees of freedom which have an influence on the observed velocity flux distributions. As far as ground state potential surfaces are concerned there have been numerous theoretical investigations on adsorption phenomena using different quantum chemical approaches, which range from semi-empirical up to highly correlated ab initio methods [11]. Most of these studies use cluster or slab models for simulating the surface.

Cluster calculations for small molecules on metal surfaces like CO/Pd(100) or CO/Ni(100) suffer from serious convergence problems with respect to the cluster size. In most metal oxides, on the other hand, the strong ionicity allows for a local description, at least for the metal ion. Rather small clusters are in many cases sufficient to give a quantitatively correct picture of the adsorption of for example CO and NO on an oxidic substrate. For other cases, such as e.g. NO/NiO(100), the convergence of adsorption properties with the size of the clusters is the subject of current research [12].

Recently, the first ab initio cluster calculations on the MCSCF/CI-level for NO on NiO(100) have been reported where reliable potential surfaces for excited states as well as properties like oscillator strengths have been calculated [13].

By means of these potential surfaces a first principles quantum dynamical description of the DIET (desorption induced by electronic transitions) process will be possible, whereas up to now only semi-empirical [14] or totally empirical methods are used to model the desorption process on the basis of the classical Menzel–Gomer–Redhead (MGR) model [15,16].

In the present paper we focus on a characterization of the calculated potential energy surfaces (PES) and on the influence of their characteristic features on the desorption dynamics of NO on NiO(100). The experimental results obtained for this system can be summarized as follows:

- NO is adsorbed on top of a regular nickel adsorption site and the molecular axis is tilted by 45° with respect to the surface normal, the binding energy is determined to be 0.52 eV [17].
- Desorption experiments use laser energies between 3.5 and 6.4 eV and allow for a rotationally and vibrationally state resolved detection [8].
- The existence of two maxima in the velocity flux distributions can be attributed to two non-thermal desorption channels. A coupling between the rotational and translational degrees of freedom of the desorbing molecules was found in the fast channel. The two channels show rotational temperatures of 250 to 450 K and vibrational temperatures of about 2000 K. In the system NO/NiO(111) nearly all experimental results are similar to those in NO/NiO(100), but the coupling between rotation and translation is not observed [8].
- NO^- is postulated as the most likely intermediate during desorption in order to explain the high vibrational temperature of the desorbing NO molecules [8].

2. Method of calculation

Nickel oxide crystallizes in a rock salt structure, where the Ni^{2+} and O^{2-} ions build up an fcc lattice. Each nickel cation is octahedrally surrounded by six oxygen anions and vice versa.

The NiO(100) surface is simulated by means of a NiO_5^{8-}-cluster (one Ni^{2+} ion and the five 'next neighbour' O^{2-} ions) (see Fig. 1) embedded in a semi-infinite Madelung field of point charges (± 2) to model the long range Coulomb interaction between the substrate and the adsorbate. The justification for using such a small cluster is discussed in detail in Ref. [13].

Larger clusters have also been investigated for the description of ground state properties for NO/NiO(100) [12], but are not really necessary for the excited states. On the other hand, they require large CPU times because extensive configuration interaction (CI) has to be included for a reasonable description of the excited states.

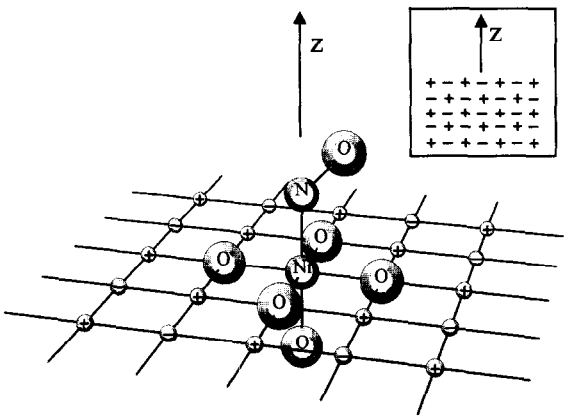

Fig. 1. The NiO_5^{8-} cluster embedded in a semi-infinite field of point charges (only the uppermost layer is shown). The adsorbate (NO) is tilted by 45° with respect to the surface normal.

The present CI calculations have been performed with the programs of the Bochum open-shell program package [18–20]. In general, we have included all fifteen O 2p, the five Ni 3d and the two NO 2π orbitals in the active space for the CI and have allowed for all single and double excitations within the valence shell, relative to the ground state reference configuration. In our previous paper [13] we have discussed different possibilities how to generate the occupied and virtual orbitals to be used in the reference configuration and in the CI. The two main choices are: (a) Frozen SCF orbitals for the ground states of NO^- and the neutral (i.e. non-ionized) cluster, as determined for the isolated subsystems and (b) CASSCF orbitals for the ground state of the cluster-NO system determined for each interaction geometry. The former method is computationally simpler and accounts for the effect that the orbitals in NO^- are different from those in NO. The description of all orbital relaxations in the cluster and in NO requires CASSCF calculations for the very highly excited charge transfer states and suffers from serious convergence problems.

Of course, both methods have the disadvantage that the relaxation of the cluster orbitals upon the transfer of one electron from the cluster to NO and the polarization of the cluster by the negative charge at NO^- and vice versa are not properly accounted for and have to be added as a semi-empirical correction. However, a similar but smaller correction for the extracluster polarization has also to be added in both of the methods. We have shown in Ref. [13] that the form of the potential curves for the charge transfer states involved in the laser desorption is not very sensitive to whether method (a) or (b) has been used. Therefore, we have applied the more adequate method (a) in the present calculations.

The basis set used in the present calculations consists of the 13s6p4d basis of Roos et al. [21] for Ni, the 7s3p basis of Huzinaga [22] contracted to double-zeta quality for the oxygen atoms of the cluster, and the 9s5p basis of Huzinaga [22] contracted to triple-zeta quality for N and O in NO. The 7s3p basis has been extended by a semidiffuse p-set with an exponent of 0.1 in order to describe the diffuse electron distribution of the oxygen anions. For similar reasons the 9s5p basis has been augmented by a diffuse p-set (exponents 0.05 for N and 0.06 for O) to allow for a better description of the NO^- intermediate.

3. Results

3.1. Characterization of potential energy surfaces

As discussed in detail before [13], we were able to identify NO^--like states (called 'charge transfer states' in the remainder of the paper) as excited states of the cluster/adsorbate system in which one electron is transferred from the cluster into the 2π-orbitals of NO. Because of the large oscillator strengths for transitions from the ground state into some of these charge transfer states it seems possible that optical transitions can lead to the intermediate NO^--like species, but also indirect excitation mechanisms (via 'hot electrons') are consistent with our calculations.

Potential energy surfaces have been constructed for these excited states with the Ni–N distance (r) and the tilt angle (α) with respect to the surface normal as internal coordinates. These two degrees of freedom have to be included since the internal NO vibration is found experimentally to be decoupled from the translation during desorption but the velocity flux distributions exhibit a strong rotation–translation coupling (see Section 1).

In Ref. [13] we have found that the PES of the NO/NiO(100) ground state has a very shallow minimum, while the PES's of the excited charge transfer states exhibit pronounced minima at $r \approx 3.5$ a.u. and a r^{-1} behaviour for larger r. At the equilibrium distance ($r = 5.0$ a.u.) of the ground state the PES's for ground and charge transfer states are quite similar as far as the tilt angle α is concerned. Such a behaviour does not allow for a straightforward interpretation of the rotation–translation coupling. Fig. 2 shows the angular dependence of the electronic ground state and that charge transfer state with the largest oscillator strength

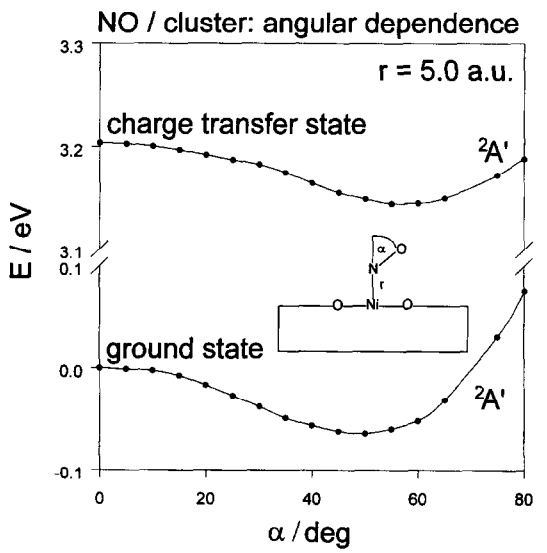

Fig. 2. Potential energy as a function of the tilt angle α for the ground state and the charge transfer state with the largest oscillator strength for a transition from the ground state. The potential curves refer to the equilibrium distance of the ground state ($r = 5.0$ a.u.).

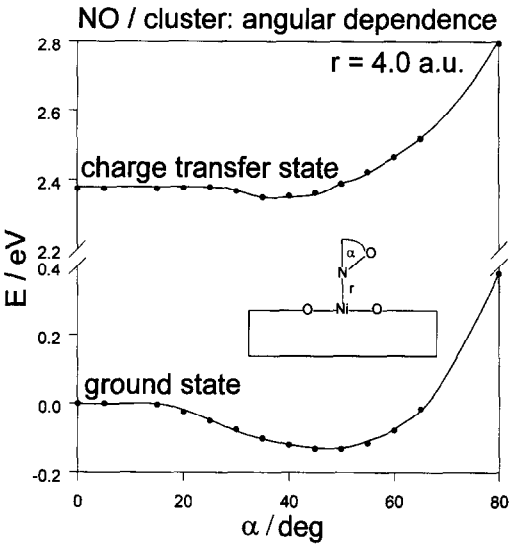

Fig. 3. Potential energy as a function of the tilt angle α for the ground state and the charge transfer state with the largest oscillator strength for a transition from the ground state. The potential curves refer to a distance of $r = 4.0$ a.u.

for transitions from the ground state. The semi-empirical correction introduced in Ref. [13] has been applied for the excitation energy.

However, the angular dependence changes dramatically for distances shorter than $r = 5.0$ a.u. In Fig. 3 the same states are shown at a distance of $r = 4.0$ a.u. The electronic ground state still prefers a tilted geometry ($\alpha \approx 50°$) while the charge transfer state is characterized by a linear adsorption geometry. This charge transfer state is a fairly high excited state of the system, therefore we had convergence problems in the CI and the shallow minimum in the potential curve might be an artifact. However, Fig. 4 shows that the preference for a linear adsorption of NO^- at short distances is even more pronounced for the lower charge transfer states which are easier to calculate and cause no convergence problems.

In order to understand the preference for a linear adsorption geometry in the charge transfer states we have analysed the Pauli-repulsion between the NO^- intermediate and the oxygen ions of the cluster. The energy contribution due

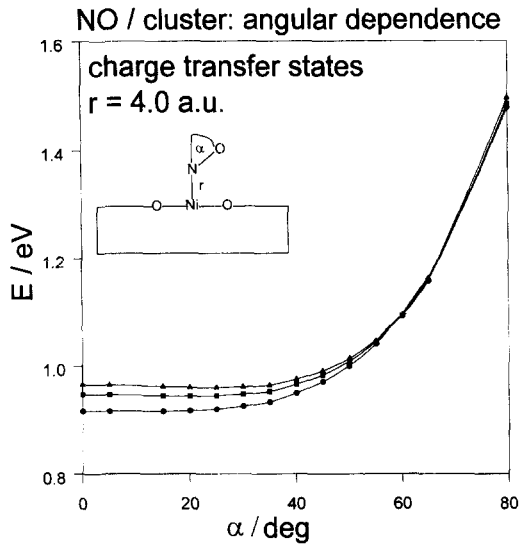

Fig. 4. Potential energy as a function of the tilt angle α for the 3 lowest charge transfer states of the same spatial symmetry as the ground state (A'), $r = 4.0$ a.u.

to the Pauli repulsion at a given geometry r and α can be obtained as follows:

$$E_{\text{pauli}(r,\alpha)} = E^{NO^-}_{\text{static}(r,\alpha)} - E_{\text{el}(r,\alpha)}$$
$$= E^{NO^-}_{\text{static}(r,\alpha)} - E^{NO^-}_{\text{Mad}(r,\alpha)} - E^{\text{dipol}}_{\text{artif}(r)}$$

where $E^{NO^-}_{\text{static}(r,\alpha)}$ is the (static) expectation value of NO^- above the NiO_5^{8-}-cluster in the Madelung field (relative to the energy at infinite cluster/NO^- distance) and static means that the frozen wave functions for the isolated NO^- ion as well as for the embedded cluster are used for the calculation of the expectation value. Of course, $E^{NO^-}_{\text{static}(r,\alpha)}$ contains both the electrostatic interaction $E_{\text{el}(r,\alpha)}$ between NO^- and the electrostatic field above the surface and the Pauli-repulsion between the cluster and the NO^- at the respective geometry (r, α). The electrostatic interaction can be estimated by calculating the energy of NO^- (static Hartree Fock expectation value) in the pure point charge (Madelung) field representing the non-ionized NiO(100) surface, where ideal point charges of ± 2 are used. This interaction energy is denoted by $E^{NO^-}_{\text{Mad}(r,\alpha)}$

For the calculation of both $E^{NO^-}_{\text{static}(r,\alpha)}$ and $E^{NO^-}_{\text{Mad}(r,\alpha)}$ the wavefunction and point charge field of the non-ionized neutral cluster has been employed instead of those describing the ionized system. This is the best choice since the non-relaxed orbitals have been used in the CI calculations and it is independent of the position of the positive hole in the cluster. The Coulomb attraction between this hole and NO^- vanishes anyway in the difference $E^{NO^-}_{\text{static}(r,\alpha)} - E^{NO^-}_{\text{Mad}(r,\alpha)}$.

Unfortunately, the NiO_5^{8-}-cluster embedded in pure point charges contains an artificial dipole moment of $\approx +1.0$ a.u. which is caused by the fact that the unscreened positive charges adjacent to the O^{2-} ions in the cluster polarize these O^{2-} ions towards the crystal. We have shown in Ref. [13] that this dipole moment can be nearly completely eliminated if the next positive charges are replaced by charged effective core potentials (ECPs) which prevent the electrons of the O^{2-} ions to be strongly attracted.

Since ECPs have not been used in the present calculations we have to correct for the additional electrostatic contribution $E^{\text{dipol}}_{\text{artif}(r)}$ of this artificial dipole moment.

This contribution is calculated by comparing the energy of a point charge of $q = -1$ in the pure point charge field above the NiO(100) surface with the energy of the same point charge above the embedded cluster. The data in Table 1 show that the attraction due to the artificial dipole moment is quite large and that it is greatly reduced if the embedding is improved by the ECPs. It should be noted that the artificial dipole moment of the neutral embedded NiO_5^{8-}-cluster has to be used for this estimate, since exactly this enters into the calculated interaction energies.

Taking all these effects into account we obtain the Pauli repulsion as a function of the tilt angle α for various distances as shown in Fig. 5. At the equilibrium distance of the ground state ($r = 5.0$ a.u.) the Pauli repulsion between NO^- and the cluster is rather small and constant (0.25 eV). However, at a shorter NO^-/Ni distances ($r = 4.0$ a.u.) the Pauli repulsion is much larger (1.0–1.5 eV) and depends on the tilt angle in such a way that the linear adsorption geometry is strongly preferred.

Table 1
Energy of a point charge $q = -1$ in the electrostatic field above the NiO(100) surface

r (a.u.)	E (a.u.) (PC) [a]	E (a.u.) (cluster/PC) [b]	E (eV) (artificial) [c]	E (a.u.) (cluster/ECP/PC) [d]
2.0	−0.31499	−0.43689	−3.317	−0.34928
2.5	−0.17372	−0.25878	−2.315	−0.17937
3.0	−0.09739	−0.16831	−1.930	−0.09721
3.5	−0.05506	−0.11655	−1.673	−0.05339
4.0	−0.03129	−0.08500	−1.462	−0.02921
4.5	−0.01786	−0.06488	−1.280	−0.01575
5.0	−0.01025	−0.05144	−1.121	−0.00826
5.5	−0.00594	−0.04207	−0.983	−0.00410
6.0	−0.00348	−0.03525	−0.865	−0.00181
7.0	−0.00129	−0.02607	−0.674	0.00010
8.0	−0.00058	−0.02020	−0.534	0.00061
9.0	−0.00034	−0.01612	−0.429	0.00067
10.0	−0.00025	−0.01315	−0.351	0.00063
15.0	−0.00016	−0.00585	−0.155	0.00033
20.0	−0.00011	−0.00324	−0.085	0.00019
30.0	−0.00005	−0.00140	−0.037	0.00009
40.0	−0.00002	−0.00077	−0.020	0.00006
50.0	−0.00001	−0.00049	−0.013	0.00004
100.0	0.00000	−0.00013	−0.004	0.00000
5000.00	0.00000	0.00000	0.000	0.00000

[a] Pure point charge field.
[b] NiO_5^{8-} cluster embedded in the pure point charge field.
[c] Contribution due to the artificial dipole moment.
[d] NiO_5^{8-} embedded in 13 effective core potentials and the point charge field.

Since our estimate for the contribution of the artificial dipole moment does not depend on α, the data in Fig. 5 should only be regarded as a first guess. If the α-dependence of $E_{\text{artif(r)}}^{\text{dipol}}$ would be included, the trend towards a stronger Pauli repulsion at tilted geometries would even be more pronounced since for $\alpha > 0$ the effective Ni–N distance becomes smaller and the Pauli repulsion is stronger.

Therefore the difference in the behaviour of the ground state and the charge transfer states with respect to the tilt angle can be understood as being due to an α-dependent increase of Pauli repulsion in the charge transfer states. The consequences of this behaviour on the dynamics of the NO desorption will be discussed in Section 4.

3.2. Characterization of the excitation process

A second aspect which has not been addressed so far is the question whether Ni or O is preferably ionized in the charge transfer from the cluster to the NO-molecule. It is possible to answer this question by an analysis similar to the one in the previous section.

This analysis is performed for the linear adsorption of NO on NiO(100), i.e. for $\alpha = 0°$, and as a function of the Ni–N distance r. First, the Pauli repulsion between NO^- and the cluster has been calculated by the same procedure as described above. Secondly, the electrostatic contribution to the total energies of the charge transfer states is modelled by the interaction of NO^- with different point charge (Madelung) fields which are designed to simulate the ionization from either the Ni or the O atoms. In these models the energies of the charge transfer states are calculated as energy expectation values of the NO^- anion in the modified point charge fields, using the unmodified wave function of the isolated NO^- ion.

The first model (field 1) describes the situation in which the electron is transferred from Ni^{2+} to NO by just replacing the point charge of the Ni^{2+} cation at the adsorption site by +3

and keeping the remainder of the point charge field unchanged.

The ionization out of the O^{2-} ions has been described using two different models. In the first one only those point charges of the Madelung field have been modified which represent the surface oxygen ions within the NiO_5^{8-}-cluster (field 2). At these positions the effective negative charge of the 'neutral' field has each been reduced by 0.25. Similarly, an ionization from an orbital delocalized over all oxygen ions is modelled by a reduction of the effective charges at the positions of the five cluster oxygen ions by 0.2 (field 3).

The resulting potential energy curves obtained by adding the Pauli repulsion to these simulations of different Coulomb interactions are shown in Fig. 6 together with the potential energy curve obtained by the CI calculations described in Section 2.

The results of this analysis clearly show that the best agreement between the ab initio CI potential curve and the simulated potential curves is obtained for the ionization from the oxygen ions (either the surface oxygen ions or all cluster oxygen ions). The potential curve for the ionization from Ni deviates very strongly

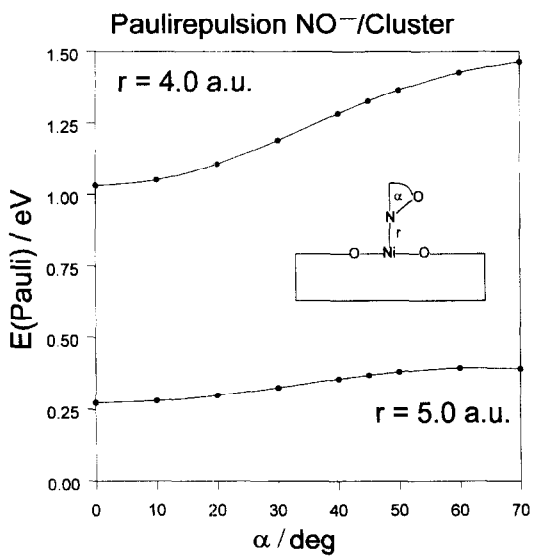

Fig. 5. Pauli repulsion for an NO^--molecule above the NiO_5^{8-} cluster as function of the tilt angle α for two selected distances.

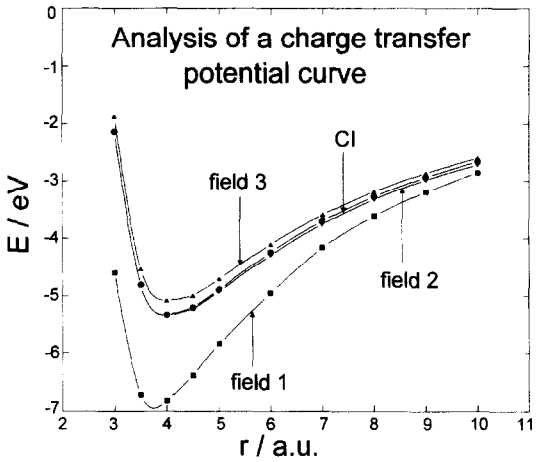

Fig. 6. Analysis of a charge transfer potential curve for a linear adsorption geometry (r denotes the Ni–N distance). Fields 1, 2 and 3 simulate different electrostatic situations after electron transfer: field 1: ionization out of Ni, field 2: ionization out of surface oxygens of the cluster and field 3: ionization out of all oxygen atoms of the cluster. CI denotes the ab initio calculated potential curve.

from the ab initio curve. Therefore we conclude that the charge transfer states presented in this paper describe an electron transfer from the oxygen-atoms of the cluster to the NO molecule.

This conclusion could be slightly modified if extra- and intracluster polarization effects after the ionization of the cluster are included in the CI calculations. This problem has been addressed in Ref. [13] in detail. Polarization and relaxation effects in the final (= ionic states) result in a stronger mixing of O and Ni orbitals and can lead to an additional contribution of the Ni3d orbitals to the charge transfer. Of course, if the extra- and intracluster polarization effects are taken into account also our semi-empirical correction of the vertical excitation energies has to be modified. Our estimate of 5 eV might be too large, because it is obtained for a local ionization out of a Ni-ion [13] and leads to a slight underestimation of vertical excitation energies.

4. Conclusions

The results presented in the Section 3 are of general interest as far as the mechanism of the

desorption dynamics of the NO/NiO-system is concerned. First of all, they support the assumption that NO^- is the intermediate during laser induced desorption [8]. This is in contrast to the results of Zimmermann et al. reported in a recent review [1], that only a very limited charge transfer from the substrate to the NO molecule takes place for metals as well as for oxide surfaces. The present analysis of the charge transfer states derived from high quality ab initio calculations clearly shows that NO^- is the intermediate during laser induced desorption from NiO(100) and that the electron transfer can be described by an ionization of the oxygen 2p-orbitals of the cluster.

Additionally, the analysis of the charge transfer potential energy surfaces yields some new information on the dynamics of the laser induced desorption, so that a rather detailed picture of the nuclear motion of NO^- above the NiO(100) surface is possible. As a result of the Coulomb attraction between NO^- and the hole created within NiO, the NO^- molecule is accelerated towards the surface directly after the charge transfer excitation. As soon as NO^- approaches the surface, it will prefer an upright adsorption geometry because of the increasing NO^-/O^{2-} Pauli repulsion for tilted NO^-. This leads to an angular torque and causes a rotational excitation of the NO^- ion. This property of the potential surfaces in the excited states offers a qualitative explanation of the rotation/translation coupling observed experimentally in the fast channel of the velocity flux distributions of the system NO/NiO(100): molecules desorbing with high velocities are also rotationally excited.

The key property is the mean lifetime of the molecules in the excited state. The longer the intermediate lives the closer the NO^- ion can approach the surface and the more kinetic energy is gained because of the strong Coulomb attraction. Simultaneously, a longer lifetime results in a greater rotational excitation because of the increase of the Pauli repulsion with decreasing distance for a tilted NO^-, so that the molecule is accelerated towards an upright position.

Another experimental detail might also be understood in this qualitative picture. The coupling between rotation and translation is only observed for the NiO(100) and not for the NiO(111) surface. Since NiO(111) is a polar surface the Pauli repulsion an approaching NO^- will feel with respect to a variation of the tilt angle is more isotropic because of O^{2-} not being present in the uppermost layer of the surface. So far, calculations for the NiO(111) surface have not been performed but we think that it is plausible to explain the differences in the velocity flux distributions of the two systems in such a way.

In order to quantitatively simulate the velocity flux distributions three dimensional wave packet calculations using the present ab initio potential surfaces will be performed in future [23]. Up to now only one dimensional wave packet calculations have been performed [24]. They yield a mean lifetime of the intermediate between 15 fs and 25 fs showing that NO^- approaches the surface to about 3.5 a.u. (the equilibrium distance of the ground state is about 5.0 a.u.), so that the present analysis of the potential energy surfaces has been carried out in that region (at $r = 4.0$ a.u.) which is most important for the desorption process.

Acknowledgements

The work was financially supported by the Deutsche Forschungsgemeinschaft through the Graduiertenkolleg 'Dynamische Prozesse an Festkörperoberflächen', the Ministerium für Wissenschaft und Forschung des Landes Nordrhein-Westfalen, the German-Israeli Foundation (GIF) and the Studienstiftung des deutschen Volkes.

References

[1] F.M. Zimmermann and W. Ho, Surf. Sci. Rep. 22 (1995) 127.

[2] F. Träger, in: P. Hess (Ed.), Photothermal and Photochemical Processes at Surfaces and Thin Films, Topics in Current Physics, Vol. 47 (Springer-Verlag, Berlin, 1993).
[3] R.R. Cavanagh, D.S. King, J.C. Stephenson and T.F. Heinz, J. Phys. Chem. 97 (1993) 786.
[4] X.L. Zhou, X.Y. Zhu and J.M. White, Surf. Sci. Rep. 13 (1991) 77.
[5] H.L. Dai and W. Ho (Eds.), Laser Spectroscopy and Photochemistry on Metal Surfaces, Adv. Ser. Phys. Chem. 5 (World Scientific Publishing Co., Singapore, 1995).
[6] K. Al-Shamery, M. Menges, I. Beauport, B. Baumeister, T. Klüner, Th. Mull, H.-J. Freund, C. Fischer, P. Andresen, J. Freitag, and V. Staemmler, Proc. SPIE'S OE/Laser '94 Conference (1994) p. 2125.
[7] W. Ho, Surf. Sci. 299–300 (1994) 996.
[8] M. Menges, B. Baumeister, K. Al-Shamery, H.-J. Freund, C. Fischer and P. Andresen, J. Chem. Phys. 101 (1994) 3318.
[9] M. Asscher, F.M. Zimmermann, L.L. Springsteen, P.L. Houston and W. Ho, J. Chem. Phys. 96 (1991) 4808.
[10] I. Beauport, K. Al-Shamery and H.-J. Freund, Chem. Phys. Lett. 256 (1996) 641.
[11] J. Sauer, P. Ugliengo, E. Garrone and V.R. Saunders, Chem. Rev. 94 (1994) 2095.
[12] M. Pöhlchen, T. Klüner, J. Wasilewski and V. Staemmler, to be published.
[13] T. Klüner, H.-J. Freund, J. Freitag and V. Staemmler, J. Chem. Phys. 104 (1996) 10030.
[14] D.R. Jennison, E.B. Stechel and A.R. Burns, J. Electron Spectrosc. Relat. Phenom. 72 (1995) 9.
[15] D. Menzel and R. Gomer, J. Chem. Phys. 41 (1964) 3311.
[16] P.A. Redhead, Can. J. Phys. 42 (1964) 886.
[17] H. Kuhlenbeck, G. Odörfer, R. Jaeger, G. Illing, M. Menges, Th. Mull, H.-J. Freund, M. Pöhlchen, V. Staemmler, S. Witzel, C. Scharfschwerdt, K. Wennemann, T. Liedtke and M. Neumann, Phys. Rev. B 43 (1991) 1969.
[18] V. Staemmler, Theor. Chim. Acta 45 (1977) 89.
[19] U. Meier and V. Staemmler, Theor. Chim. Acta 76 (1989) 95.
[20] J. Wasilewski, Int. J. Quantum Chem. 36 (1989) 503.
[21] B. Roos, A. Veillard, and G. Vinot, Theor. Chim. Acta 20 (1971) 1.
[22] S. Huzinaga, Approximate Atomic Functions, I. (Preprint, University of Alberta, Canada, 1971).
[23] T. Klüner, R. Kosloff, V. Staemmler and H.-J. Freund, to be published.
[24] T. Klüner, Diplomarbeit, Ruhr-Universität Bochum (1994).